

Mean-field ansatz for topological phases with string tensionSébastien Dusuel^{1,*} and Julien Vidal^{2,†}¹*Lycée Saint-Louis, 44 Boulevard Saint-Michel, 75006 Paris, France*²*Laboratoire de Physique Théorique de la Matière Condensée, CNRS UMR 7600, Université Pierre et Marie Curie, 4 Place Jussieu, 75252 Paris Cedex 05, France*

(Received 10 June 2015; revised manuscript received 11 September 2015; published 29 September 2015)

We propose a simple mean-field ansatz to study phase transitions from a topological phase to a trivial phase. We probe the efficiency of this approach by considering the string-net model in the presence of a string tension for any anyon theory. Such a perturbation is known to be responsible for a deconfinement-confinement phase transition which is well described by the present variational setup. We argue that mean-field results become exact in the limit of large total quantum dimension.

DOI: [10.1103/PhysRevB.92.125150](https://doi.org/10.1103/PhysRevB.92.125150)

PACS number(s): 75.10.Jm, 05.30.Pr, 05.30.Rt, 71.10.Pm

I. INTRODUCTION

The blend of quantum computation and of topological phases of matter [1] have led to the idea of topological quantum computation [2–4]. In this field, the essential ingredient is the construction of physical systems sustaining exotic excitations known as non-Abelian anyons (see Ref. [5] for a review). Being genuinely nonlocal, these anyons allow for efficient storage and manipulation of quantum information. Indeed, topologically ordered systems [1] are stable under local perturbations [6] and hence protected against undesirable effects such as decoherence. However, strong enough perturbations, may drive the system to a nontopological phase. In recent years, many works have been devoted to the study of this robustness in microscopic models. Such an issue is difficult to address since one has to deal with two-dimensional interacting quantum systems and the complex nature of the anyonic quasiparticles prevents one from using standard methods.

The goal of the present work is to propose a simple approach that may be considered as a mean-field theory for topological phases. To this end, we introduce a variational ansatz which can describe topological as well as nontopological phases. By construction, it also matches the exact ground state in some limiting cases. Thus, it aims at qualitatively describing phase diagrams while being quantitatively acceptable. Most models hosting topological quantum order are built as a sum of local commuting projectors (toric code [2], string nets [7], . . .). In lattice gauge theories, one often interprets these projectors as operators measuring effective fluxes and charges. The topologically ordered ground state (vacuum) is then defined as the flux-free and charge-free state. Elementary excitations are obtained by locally violating this constraint. In two dimensions, excitations are pointlike anyons related by strings and their energy does not depend on their relative position so that topological phases are also called deconfined phases. A natural way to destroy topological order consists in adding a string tension that will drive the system to a confined phase. The prototypical Hamiltonian of such a system can be

written

$$H = -J_v \sum_v Q_v - J_p \sum_p B_p - J_l \sum_l L_l, \quad (1)$$

where Q_v (B_p) are projectors measuring charges (fluxes) on vertices (plaquettes) of a two-dimensional graph and where L_l is an operator acting on links which induces a string tension. In the following, we consider a two-dimensional plane with open boundary conditions so that the ground state is unique in the thermodynamical limit. Assuming non-negative couplings, the ground state of H is readily written in two limiting cases. On one hand, in the trivial phase $J_v = J_p = 0$, the ground state is a (polarized) product state denoted by $|0\rangle$, where all links are in the same state. On the other hand, for $J_l = 0$, the ground state is proportional to $\prod_v Q_v \prod_p B_p |0\rangle$. The main idea of our construction is to find a simple variational state that bridges the gap between these two extreme cases.

In this paper, we focus on the string-net model in the honeycomb lattice since it allows one to study a wide variety of topological phases [7,8]. Interested readers that are not familiar with this model can find a detailed study of this variational approach in the simpler case of the toric code model in Appendix B.

The string-net Hamiltonian [7] is a special case of Eq. (1) where the operator B_p favors the zero-flux configuration in plaquette p . Here, we only consider states without charge excitation so that the Hilbert space is spanned by all link configurations satisfying the so-called branching rules (stemming from the fusion rules of the considered anyon theory). We thus drop the $-J_v \sum_v Q_v$ term in the Hamiltonian. For simplicity, we also restrict our discussion to the string tension term introduced in Ref. [9] which involves L_l operators enforcing a zero flux in link l of the lattice. Operators B_p and L_l commute except if link l belongs to plaquette p .

II. ANSATZ STATE AND ITS BASIC PROPERTIES

To describe the phase transition separating the topological phase from the trivial phase, we introduce the following single-parameter variational state:

$$|\alpha\rangle = \mathcal{N} \prod_p (\mathbb{1} + \alpha Z_p) |0\rangle, \quad (2)$$

*sdusuel@gmail.com

†vidal@lptmc.jussieu.fr

where $0 \leq \alpha \leq 1$, and $Z_p = 2B_p - \mathbb{1}$ is such that $Z_p^2 = \mathbb{1}$. The normalization constant \mathcal{N} depends on the total quantum dimension D of the theory considered, on α , and on the system size (see Appendix A). Once again, the physical insight underlying this ansatz is that $|\alpha = 0\rangle = |0\rangle$ is the exact ground state for $J_p = 0$, while $|\alpha = 1\rangle \propto \prod_p B_p |0\rangle$ is the exact ground state for $J_l = 0$. Thus, one can expect that it captures the physics, at least qualitatively, for nonvanishing couplings.

Interestingly, the structure of $|\alpha\rangle$ implies that for any set \mathcal{P}_n of n plaquettes, one has

$$\left\langle \prod_{p \in \mathcal{P}_n} B_p \right\rangle_\alpha = \prod_{p \in \mathcal{P}_n} \langle B_p \rangle_\alpha = \left[\frac{(1 + \alpha)^2}{D^2(1 - \alpha)^2 + 4\alpha} \right]^n, \quad (3)$$

where $\langle \mathcal{O} \rangle_\alpha = \langle \alpha | \mathcal{O} | \alpha \rangle$ (see Appendix A for details). This factorization property reveals the mean-field character of $|\alpha\rangle$. In addition, for Abelian theories, $|\alpha\rangle$ can be rewritten as a simple product state in the dual plaquette (flux) basis. For illustration, let us consider the simplest Abelian theory, i.e., \mathbb{Z}_2 ($D^2 = 2$). As shown in Ref. [10], for this theory, the string-net model with a string tension can be mapped onto the transverse-field Ising model on the triangular lattice by setting $X_p X_{p'} = 2L_l - \mathbb{1}$, where p and p' are plaquettes sharing link l . In this dual representation, degrees of freedom are defined on plaquettes (instead of links) and operators X_p and Z_p are the usual Pauli matrices. One can then compute the following expectation values in the link basis (see Appendix A)

$$\langle 2B_p - \mathbb{1} \rangle_\alpha = \frac{2\alpha}{1 + \alpha^2}, \quad \langle 2L_l - \mathbb{1} \rangle_\alpha = \left(\frac{1 - \alpha^2}{1 + \alpha^2} \right)^2, \quad (4)$$

and in the plaquette basis

$$\langle Z_p \rangle_\theta = \cos \theta, \quad \langle X_p X_{p'} \rangle_\theta = \sin^2 \theta = \langle X_p \rangle_\theta \langle X_{p'} \rangle_\theta. \quad (5)$$

Here, we set $|\theta\rangle = \otimes_p [\cos(\theta/2)|\uparrow\rangle_p + \sin(\theta/2)|\downarrow\rangle_p]$ where $|\uparrow\rangle_p$ and $|\downarrow\rangle_p$ are the eigenstates of Z_p with eigenvalues $+1$ and -1 . Clearly, expressions (4) and (5) coincide provided $\alpha = \tan(\theta/2)$.

The \mathbb{Z}_N case can be treated similarly by mapping the model onto the transverse-field N -state Potts model [10] (other models with \mathbb{Z}_2 and \mathbb{Z}_3 topological order have also been treated in the same vein [11–13]). Although no such mapping is known for non-Abelian theories (because of the existence of multiple fusion channels), the state $|\alpha\rangle$ can still be considered as a mean-field ansatz because of the factorization property (3). In other words, the present approach generalizes the canonical mean-field treatment (performed in the dual basis) implemented for Abelian anyons, to non-Abelian theories.

III. RESULTS

For any theory with total quantum dimension D , one can compute the variational energy per plaquette

$$e(\alpha) = - \frac{J_p f_p(\alpha) + 3J_l f_l(\alpha)}{g(\alpha)}, \quad (6)$$

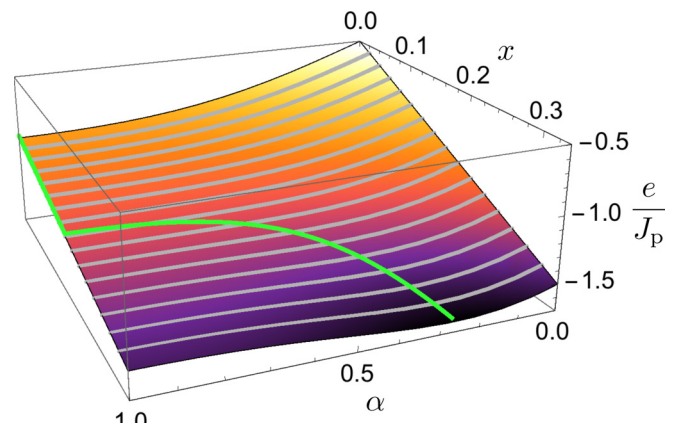


FIG. 1. (Color online) Energy landscape as a function of α and $x = J_l/J_p$ for $D^2 = 2$. The green line shows the position of the absolute minimum $\alpha(x)$. In this case, the transition is found to be continuous (second order).

where

$$g(\alpha) = D^2[D^2(1 - \alpha)^2 + 4\alpha]^2, \quad (7)$$

$$f_p(\alpha) = D^2(1 + \alpha)^2[D^2(1 - \alpha)^2 + 4\alpha], \quad (8)$$

$$f_l(\alpha) = D^6(1 - \alpha)^4 + 8D^4\alpha(1 - \alpha)^3 + 24D^2\alpha^2(1 - \alpha)^2 + 16\alpha^3(2 - \alpha). \quad (9)$$

Details of the calculations are given in Appendix A. Setting $x = J_l/J_p$, the study of $e(\alpha)$ indicates that the system undergoes a phase transition at $x_c = \frac{D^2 - 1}{3D^2}$. Indeed, the minimum of e is obtained for $\alpha_- = 1$ if $x \leq x_c$ and for $\alpha_+ \leq 1$ if $x \geq x_c$ (see Figs. 1 and 2 for illustration). This transition is second order for $D^2 = 2$ only, and first order for $D^2 > 2$. At the transition, one has $\alpha_+(x_c) = \frac{D^2}{3D^2 - 4}$.

Interestingly, all these variational results only depend on D . This is reminiscent of the intrinsically local character of the ansatz that does not take into account subtle effects due to

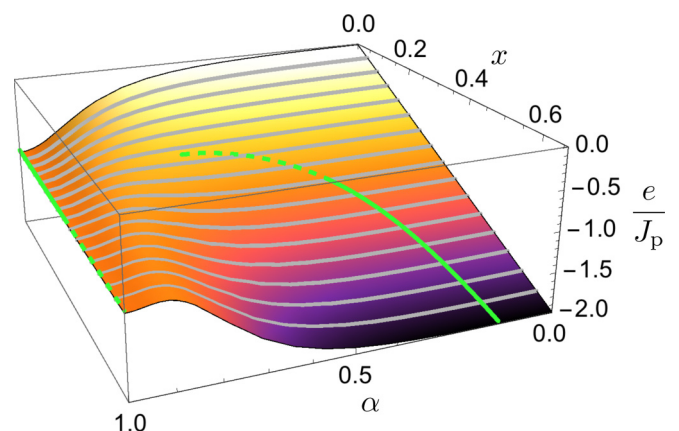


FIG. 2. (Color online) Energy landscape as a function of α and $x = J_l/J_p$ for $D^2 = 100$. The green (dotted) line shows the position of the absolute (local) minimum $\alpha(x)$. For $D^2 > 2$, the transition is found to be discontinuous (first order).

nontrivial braiding statistics. Within this mean-field approach (single-plaquette approximation), two theories with the same total quantum dimension D are thus treated on an equal footing. Nevertheless, from high-order series expansions, we know that, for instance, \mathbb{Z}_4 and Ising theories ($D^2 = 4$) have different ground-state energies [14].

Consequently, it is natural to wonder how these predictions compare with exact results. First, it is worth noting that, in the topological phase ($x < x_c$), the energy is minimized for $\alpha = 1$ which is the exact result for $x = 0$. For $\alpha = 1$, the ground-state energy reads

$$\frac{e(\alpha_-)}{J_p} = -1 - \frac{3x}{D^2}, \quad (10)$$

which matches the exact small- x perturbative expansion up to order 1 but does not give higher-order corrections. Secondly, in the opposite (large- x) limit, the variational energy per plaquette can be expanded in powers of $1/x$ and reads, at order 4,

$$\begin{aligned} \frac{e(\alpha_+)}{J_l} = & -3 - \frac{1}{x} \frac{1}{D^2} - \frac{1}{x^2} \frac{D^2 - 1}{6D^4} - \frac{1}{x^3} \frac{D^4 - 3D^2 + 2}{36D^6} \\ & - \frac{1}{x^4} \frac{2D^6 - 11D^4 + 19D^2 - 10}{432D^8}. \end{aligned} \quad (11)$$

This expansion matches the exact large- x series expansion up to order 3 but not beyond. Once again, this is due to the local character of the ansatz that does not capture quantum fluctuations beyond a single plaquette.

Another important remark concerns the behavior of the so-called Wilson loop operators denoted $W_{C_n}^s$ for a contour C_n enclosing n plaquettes and a string of type s (see Appendix A). In the deconfined (confined) phase, the expectation value of $W_{C_n}^s$ is expected to scale as the perimeter (area) of C_n [19]. Remarkably, the present mean-field approach displays this behavior since

$$\langle W_{C_n}^s \rangle_\alpha = \kappa_s d_s \left[\frac{4\alpha}{D^2(1-\alpha)^2 + 4\alpha} \right]^n, \quad (12)$$

where κ_s and d_s are the Frobenius-Schur indicator and the quantum dimension of the string s , respectively (see Appendix A). In the topological phase, one has $\langle W_{C_n}^s \rangle_{\alpha_-} = \kappa_s d_s$ for any C_n , which can be interpreted as a trivial perimeter law with an infinite characteristic length. By contrast, in the polarized phase, one has $\langle W_{C_n}^s \rangle_{\alpha_+} = \kappa_s d_s e^{-n/\mathcal{A}}$ where the characteristic area \mathcal{A} is readily obtained from Eq. (12).

Let us now compare the mean-field predictions with existing results. As explained above, for the \mathbb{Z}_N theory ($D^2 = N$), the model is equivalent to the N -state Potts model in a transverse field on the triangular lattice. This model is known to display a second-order transition (Ising universality class) for $N = 2$, and a first-order transition for $N \geq 3$ (see Ref. [20] for a review). Thus, the present mean-field treatment gives the correct order of the transition. In Table I, we give the position of the transition point x_c obtained from series expansions and from the present mean-field ansatz. Quantitatively, the difference between the results of both approaches decreases as D^2 increases. For the Potts model, the mean-field theory is even known to be exact for large

TABLE I. Position of the transition point for several theories computed with the mean-field ansatz (2) and with series expansions.

	\mathbb{Z}_2	\mathbb{Z}_3	Fibonacci	Ising
D^2	2	3	3.618	4
x_c (mean field)	0.1667	0.2222	0.2412	0.25
x_c (series)	0.2097 [15]	0.2466 [16]	0.256 [17]	0.261 [18]

$D^2 = N$ [21]. In this limit, one obtains a first-order transition at $x_c = 1/3$. Since $e(\alpha)$ only depends on D , this large- D mean-field result is expected to hold for all theories.

However, for non-Abelian theories with finite D , the situation is more complex. In two recent studies [17,18], using series expansion and exact diagonalizations, it has been claimed that the phase transition for Fibonacci and Ising theories is second order but the present mean-field approach predicts a first-order transition ($D^2 > 2$). Although none of these methods are exact, we strongly believe that a (weakly) first-order scenario is correct. Apart from the mean-field result, this conclusion relies on two observations which have been overlooked.

The first one relies on strong similarities of the ground-state energy series expansions between \mathbb{Z}_3 , Fibonacci, and Ising theories (see Fig. 3). In particular, a jump in the first derivative of the ground-state energy per plaquette $\partial e/\partial x$ is observed at the transition. This jump was considered as an artifact due to a finite-order series in Refs. [17,18]. As can be seen in Fig. 3, the magnitude of this jump is found to increase with D , in agreement with the mean-field result which yields

$$\left. \frac{\partial e}{\partial x} \right|_{x=x_c^-} - \left. \frac{\partial e}{\partial x} \right|_{x=x_c^+} = \frac{3(D^2 - 2)^2}{D^2(D^2 - 1)}. \quad (13)$$

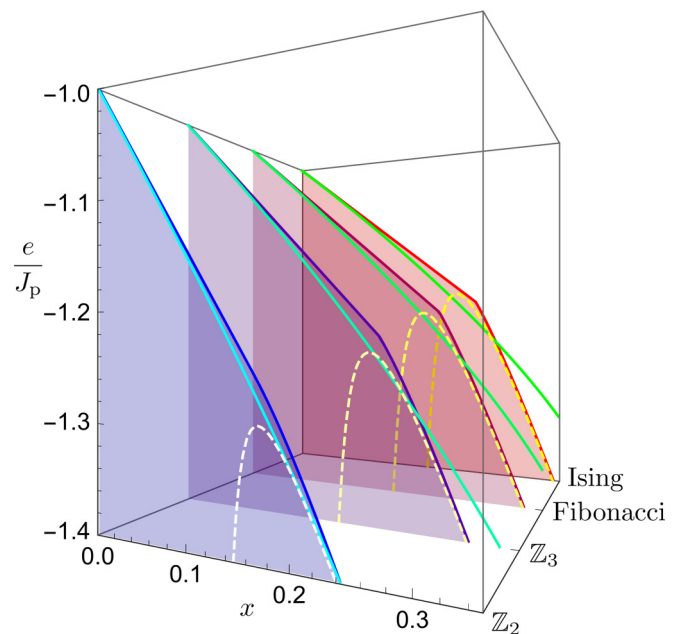


FIG. 3. (Color online) Comparison of variational results (upper boundaries of shaded planes) with low- (high-) field series expansions shown in full (dashed) lines for theories discussed in Table I. Bare series at highest available orders [15–18] are displayed.

In addition, for $D^2 > 2$, the (relative) height of the energy barrier at $x = x_c$ between the two minima α_{\pm} and the local maximum α^* reads

$$\frac{e(\alpha_{\pm}) - e(\alpha^*)}{e(\alpha_{\pm})} = \frac{D^4 - 4D^2\sqrt{D^2 - 1} + 4D^2 - 4}{4(D^4 + D^2 - 1)}. \quad (14)$$

In the limit $(D^2 - 2) \ll 1$, this relative energy vanishes as $(D^2 - 2)^4$, indicating a weakly first-order transition. Such a behavior qualitatively explains why the transition for Fibonacci and Ising theories has been considered as second order in Refs. [17,18].

The second argument that corroborates this scenario is based on the emergence of bound states in the low-energy spectrum inside the topological phase and will be discussed elsewhere. Let us simply mention that such bound states are necessary although not sufficient to induce a first-order transition and they are present for $D^2 > 2$.

The mean-field approximation can also be used to analyze the same model but in the ladder geometry for which several exact results are known [9,22–24]. In this one-dimensional case, the variational energy is straightforwardly obtained from (6) by merely replacing J_l by $J_l/3$. As for the two-dimensional case, the ansatz (2) predicts a second-order transition for $D^2 = 2$ and a first-order transition for $D^2 > 2$ although, for the ladder, the transition is known to be first order only if $D^2 > 4$ [24]. Thus, the ansatz fails at describing the nature of the transition for $D^2 \leq 4$, as already known for the Potts model [20]. Interestingly, the position of the mean-field transition point $x_c^{\text{ladder}} = \frac{D^2-1}{D^2}$ goes to 1 (self-dual point) in the large- D limit, which is the exact result for any D [24].

IV. CONCLUSION

To conclude, we would like to give some possible routes to go beyond the present approach. In Refs. [25,26], the ground state of the string-net model without string tension has been written as a tensor-network state (TNS), involving a triple-line structure (that reduces to a double-line structure for Abelian theories). Following the steps detailed in these works, the state $|\alpha\rangle$ could be written in the same way. The parameter α would only change the values taken by the tensors. Since $|\alpha\rangle$ already captures semiquantitatively the physics of the transition induced by string tension, it seems reasonable to assume that performing a minimization over all parameters of the tensors should give more precise results. The first-order nature of the phase transition for $D^2 > 2$ should furthermore be favorable to the obtention of accurate results.

TNS have already been successfully used to study phase transitions in Abelian models [11,27–29]. However, they have not yet been applied to the more challenging non-Abelian models, although the principles for doing so have been laid down [30]. The technique exhibited in the present paper can be considered as a first step, even though the tensor-network structure has been bypassed. Let us emphasize that single-parameter TNS have already been proposed for \mathbb{Z}_2 models [27,29], but their single-line structure leads to qualitatively wrong results (first-order transition). To solve this problem, Gu *et al.* introduced multiparameter double-line tensors [27]. It seems that the double-line structure (or triple-line structure for

non-Abelian theories) is crucial since it encodes information about plaquettes that is necessary for an area law in the confined phase. Our single-parameter ansatz supports this conclusion.

Let us also stress that tensors must be chosen carefully, in order to allow for topological states [31–34]. For the toric code in a parallel magnetic field, we have shown (see Appendix B for a detailed calculation) that the topological entropy [35,36] vanishes for $\alpha < 1$, i.e., in the polarized phase, but is equal to $-\log_2 D$ (which is equal to -1 since $D = 2$) for $\alpha = 1$, i.e., in the topological phase. We conjecture that the same relations hold for the string-net model, for any theory. We leave the calculation of the topological entropy, or of other measures [37,38] for future works.

The use of TNS would furthermore allow one to study other transitions. For instance, for the Fibonacci theory [17], the ground state for $J_p = 0$ and $J_l < 0$ is the state $|1\rangle$ where all links carry a string 1, namely, a Fibonacci anyon. The transition from the string-net ground state to this state could thus be studied with a variational state $|\alpha\rangle = \mathcal{N} \prod_p (\mathbb{1} + \alpha Z_p)|1\rangle$. However, analytical calculations are much harder in this case, so that numerical TNS methods would be extremely valuable.

Finally, let us mention that it would be interesting to describe excitations in a variational setting and thus to study dynamical properties in the model, as was done in Ref. [39]. We hope the present work will trigger such studies.

ACKNOWLEDGMENT

We thank F. J. Burnell, R. Orús, K. P. Schmidt, M. D. Schulz, and S. H. Simon for fruitful discussions.

APPENDIX A: STRING-NET MODEL WITH STRING TENSION

1. Definitions

The Hamiltonian of the string-net model with a string tension is given by

$$H = -J_p \sum_p B_p - J_l \sum_l L_l, \quad (A1)$$

where the string-tension operator L_l is the projector onto the trivial state $|0\rangle_l$ on the link l . The operator B_p enforcing trivial flux in plaquette p is written as $B_p = \frac{1}{D^2} \sum_s \tilde{d}_s B_p^s$. Here, we introduce $\tilde{d}_s = \kappa_s d_s$, which is the product of the Frobenius-Schur indicator κ_s and of the quantum dimension d_s of the string s . The total quantum dimension is defined as $D = \sqrt{\sum_s d_s^2}$. The operator B_p^s inserts a string s in the links of plaquette p as defined in Appendix C of Ref. [7]. Since B_p^0 acts as the identity on states satisfying branching rules (to which we restrict ourselves), we shall single it out and write $B_p^0 = \mathbb{1}$. We introduce the operator $Z_p = 2B_p - \mathbb{1}$ that satisfies $Z_p^2 = \mathbb{1}$ since B_p is a projector. With these notations and noting that $\tilde{d}_0 = 1$, one obtains

$$Z_p = -\frac{D^2 - 2}{D^2} \mathbb{1} + \frac{2}{D^2} \sum_{s \neq 0} \tilde{d}_s B_p^s. \quad (A2)$$

2. Normalization of $|\alpha\rangle$

We consider the variational state

$$|\alpha\rangle = \mathcal{N} \prod_p (\mathbb{1} + \alpha Z_p) |0\rangle, \quad (\text{A3})$$

where $0 \leq \alpha \leq 1$ is a variational parameter. The fully polarized state $|0\rangle$ is defined as $|0\rangle = \otimes_l |0\rangle_l$. The first task is to compute the normalization constant \mathcal{N} . To this end, let us note that

$$(\mathbb{1} + \alpha Z_p)^2 = (1 + \alpha^2)(\mathbb{1} + \eta Z_p), \quad \text{with} \quad \eta = \frac{2\alpha}{1 + \alpha^2}. \quad (\text{A4})$$

Thus, denoting N_p the number of plaquettes and since all B_p^s commute with one another, we find

$$1 = \langle \alpha | \alpha \rangle = \mathcal{N}^2 (1 + \alpha^2)^{N_p} \langle 0 | \prod_p (\mathbb{1} + \eta Z_p) | 0 \rangle. \quad (\text{A5})$$

For simplicity and since we are interested in the thermodynamical limit, let us assume open boundary conditions. Then, the only contribution to $\langle 0 | \prod_p (\mathbb{1} + \eta Z_p) | 0 \rangle$ comes from the term proportional to $\mathbb{1}$ that arises when expanding $\prod_p (\mathbb{1} + \eta Z_p)$. Indeed, the action of a $B_p^{s \neq 0}$ on $|0\rangle$, for a boundary plaquette, introduces nontrivial strings in the boundary links that cannot be compensated by any other operator $B_{p' \neq p}^s$. Using Eq. (A2), it is then easy to get the normalization condition

$$1 = \langle \alpha | \alpha \rangle = \mathcal{N}^2 (1 + \alpha^2)^{N_p} \varepsilon^{N_p}, \quad (\text{A6})$$

with

$$\varepsilon = 1 - \eta \frac{D^2 - 2}{D^2}. \quad (\text{A7})$$

3. Computation of $\langle B_p \rangle_\alpha$

Let us pick a particular plaquette p and compute $\langle B_p \rangle_\alpha = \langle \alpha | B_p | \alpha \rangle$. Since all B_p^s commute with one another, we get

$$\langle B_p \rangle_\alpha = \mathcal{N}^2 (1 + \alpha^2)^{N_p} \langle 0 | B_p \prod_{p'} (\mathbb{1} + \eta Z_{p'}) | 0 \rangle. \quad (\text{A8})$$

From the definition of Z_p , it is easy to derive the identity $B_p(\mathbb{1} + \eta Z_p) = (1 + \eta)B_p$. The prefactor of $\mathbb{1}$ in this term is $\frac{1+\eta}{D^2}$. Proceeding along the same lines as for the normalization of $|\alpha\rangle$, and using the expression of \mathcal{N} stemming from Eq. (A6), we then find

$$\langle B_p \rangle_\alpha = \frac{1 + \eta}{D^2} \frac{1}{\varepsilon}. \quad (\text{A9})$$

4. Computation of $\langle \prod_p B_p \rangle_\alpha$

Let \mathcal{P}_n be a set of n plaquettes. The same argument as above shows that all plaquettes of \mathcal{P}_n will have a contribution $\frac{1+\eta}{D^2} \frac{1}{\varepsilon}$, while other plaquettes have a contribution 1. As a consequence

$$\left\langle \prod_{p \in \mathcal{P}_n} B_p \right\rangle_\alpha = \left(\frac{1 + \eta}{D^2} \frac{1}{\varepsilon} \right)^n = \langle B_p \rangle_\alpha^n. \quad (\text{A10})$$

5. Computation of $\langle L_l \rangle_\alpha$

Let us finally turn to the computation of $\langle L_l \rangle_\alpha = \langle \alpha | L_l | \alpha \rangle$, which is a little bit more involved. We denote p_1 and p_2 the plaquettes sharing link l . Then L_l commutes with all Z_p operators, except those acting at plaquettes p_1 and p_2 . As a consequence

$$\begin{aligned} \langle L_l \rangle_\alpha &= \mathcal{N}^2 (1 + \alpha^2)^{N_p - 2} \langle 0 | (\mathbb{1} + \alpha Z_{p_1}) (\mathbb{1} + \alpha Z_{p_2}) \\ &\quad \times L_l (\mathbb{1} + \alpha Z_{p_1}) (\mathbb{1} + \alpha Z_{p_2}) \prod_{p \neq p_1, p_2} (\mathbb{1} + \eta Z_p) | 0 \rangle. \end{aligned} \quad (\text{A11})$$

As for the previous two computations, the only contribution to the matrix element $\langle 0 | \dots | 0 \rangle$ comes from the term proportional to $\mathbb{1}$ after expanding the operators. Consequently, we can already take into account the contribution of $\prod_{p \neq p_1, p_2} (\mathbb{1} + \eta Z_p)$, that is, $\varepsilon^{N_p - 2}$ as well as the expression of \mathcal{N} stemming from Eq. (A5), to write

$$\langle L_l \rangle_\alpha = \left(\frac{1}{1 + \alpha^2} \right)^2 \frac{1}{\varepsilon^2} \langle \psi | L_l | \psi \rangle, \quad (\text{A12})$$

where

$$|\psi\rangle = (\mathbb{1} + \alpha Z_{p_1}) (\mathbb{1} + \alpha Z_{p_2}) |0\rangle. \quad (\text{A13})$$

Denoting $\mathbb{1} + \alpha Z_p = \beta \mathbb{1} + \gamma C_p$, with

$$\beta = 1 - \alpha \frac{D^2 - 2}{D^2}, \quad \gamma = \frac{2\alpha}{D^2}, \quad \text{and} \quad C_p = \sum_{s \neq 0} \tilde{d}_s B_p^s, \quad (\text{A14})$$

one gets

$$|\psi\rangle = [\beta^2 \mathbb{1} + \beta \gamma (C_{p_2} + C_{p_1}) + \gamma^2 C_{p_1} C_{p_2}] |0\rangle. \quad (\text{A15})$$

Since L_l enforces a trivial ($s = 0$) flux in link l , and since C_p operators introduce nontrivial fluxes, only the first and third terms of $|\psi\rangle$ contribute to the matrix element appearing in Eq. (A12). When acting with $C_{p_1} C_{p_2}$ on $|0\rangle$, the only way to obtain a trivial flux in link l is to take the same s in C_{p_1} and in C_{p_2} . Thus, one gets all possible states with a loop s surrounding plaquette p_1 and a loop s surrounding p_2 . Since one requires the link l to be in the trivial $s = 0$ state, the weight of these states is equal to \tilde{d}_s , as can be found by using Eq. (2.23) in Ref. [40]. As a consequence, we obtain

$$\langle \psi | L_l | \psi \rangle = \beta^4 + \gamma^4 \sum_{s \neq 0} \tilde{d}_s^2 = \beta^4 + \gamma^4 (D^2 - 1), \quad (\text{A16})$$

so that

$$\langle L_l \rangle_\alpha = \left(\frac{1}{1 + \alpha^2} \right)^2 \frac{1}{\varepsilon^2} [\beta^4 + \gamma^4 (D^2 - 1)]. \quad (\text{A17})$$

6. Computation of $e(\alpha) = \langle H \rangle_\alpha / N_p$

Finally, we can compute the variational energy per plaquette

$$e(\alpha) = \frac{\langle \alpha | H | \alpha \rangle}{N_p} = -J_p \langle B_p \rangle_\alpha - 3J_l \langle L_l \rangle_\alpha, \quad (\text{A18})$$

where the factor of 3 comes from the fact that on a honeycomb lattice, the number of links is three times the number of

plaquettes. Replacing $\langle B_p \rangle_\alpha$ and $\langle L_l \rangle_\alpha$ by their expressions, and simplifying everything, one gets the energy per plaquette given in the main text. Note that for the ladder geometry [9], the link operator L_l only acts on rungs. As there are as many rungs as plaquettes, the variational energy per plaquette for the ladder reads $e^{\text{ladder}}(\alpha) = -J_p \langle B_p \rangle_\alpha - J_l \langle L_l \rangle_\alpha$.

7. Computation of $\langle W_{C_n}^s \rangle_\alpha$

For a contour C_n enclosing n plaquettes, the Wilson loop operator $W_{C_n}^s$ inserts a string s along C_n . In principle, one should consider two distinct operators, depending whether the string lies above or below the lattice. However, for our ansatz state, these operators have identical expectation values so that we denote both of them as $W_{C_n}^s$. This operator is given by $W_{C_n}^s = \kappa_s \mathcal{W}_{C_n}^s$ where $\mathcal{W}_{C_n}^s$ is the type- s simple-string operator defined in Ref. [7], and is nothing but a multiplaquette version of B_p^s . As $W_{C_n}^s$ commutes with all B_p^s operators,

$$\langle W_{C_n}^s \rangle_\alpha = \kappa_s \mathcal{N}^2 (1 + \alpha^2)^{N_p} \langle 0 | \prod_p (\mathbb{1} + \eta Z_p) \mathcal{W}_{C_n}^s | 0 \rangle. \quad (\text{A19})$$

Since $\mathcal{W}_{C_n}^s | 0 \rangle$ is the state with a string s along C_n , the only nonzero contribution comes from $(N_p - n)$ operators $\mathbb{1}$ for plaquettes outside C_n , and from n operators $B_p^{\bar{s}}$ inside C_n , annihilating the string s (where \bar{s} is the dual string of s). Each of the n fusions of s and \bar{s} gives a factor κ_s/d_s , and the resulting contractible s loop gives a factor d_s . As a result

$$\langle W_{C_n}^s \rangle_\alpha = \kappa_s \mathcal{N}^2 (1 + \alpha^2)^{N_p} \varepsilon^{N_p - n} \left(\frac{2\eta \tilde{d}_s}{D^2} \right)^n \left(\frac{\kappa_s}{d_s} \right)^n d_s. \quad (\text{A20})$$

Simplifying this expression finally yields

$$\langle W_{C_n}^s \rangle_\alpha = \kappa_s d_s \left(\frac{2\eta}{D^2 \varepsilon} \right)^n. \quad (\text{A21})$$

Let us mention that, as for a single plaquette, one can build the projector $W_{C_n} = \frac{1}{D^2} \sum_s \tilde{d}_s W_{C_n}^s$ onto flux 0 inside C_n . This operator has the following expectation value:

$$\langle W_{C_n} \rangle_\alpha = \frac{1}{D^2} \left[1 + (D^2 - 1) \left(\frac{2\eta}{D^2 \varepsilon} \right)^n \right]. \quad (\text{A22})$$

From this expression, it follows that $\langle W_{C_n} \rangle_{\alpha=1} = 1$ as expected. Furthermore, when $n = 1$, one can check that $\langle W_{C_{n=1}} \rangle_\alpha = \langle B_p \rangle_\alpha$ given in Eq. (A9). This result allows one to rewrite the expectation value of Wilson operators as

$$\langle W_{C_n}^s \rangle_\alpha = \kappa_s d_s \left(\frac{D^2 \langle B_p \rangle_\alpha - 1}{D^2 - 1} \right)^n. \quad (\text{A23})$$

APPENDIX B: TORIC CODE IN A MAGNETIC FIELD

1. Definitions

The Hamiltonian of the toric code in a magnetic field reads

$$H = -J \sum_v A_v - J \sum_p B_p - \sum_l \mathbf{h} \cdot \boldsymbol{\sigma}_l, \quad (\text{B1})$$

where $\mathbf{h} = (h_x, h_y, h_z)$ is a uniform magnetic field and $\boldsymbol{\sigma}_l = (\sigma_l^x, \sigma_l^y, \sigma_l^z)$ are Pauli operators at link l of a square lattice. Furthermore, $A_v = \prod_{l \in v} \sigma_l^x$ and $B_p = \prod_{l \in p} \sigma_l^z$, where v and p , respectively, denote vertices and plaquettes of the lattice (see Ref. [28], and references therein for a detailed discussion

of this model). These operators all commute with one another and $A_v^2 = B_p^2 = \mathbb{1}$. Note that, with these definitions, A_v and B_p are not defined as projectors. In the following, we shall only consider a system in the thermodynamical limit with open boundary conditions.

2. Ansatz and limiting cases

For a given direction of the magnetic field \mathbf{h} , following the mean-field prescription previously detailed for string nets, we introduce the following variational state:

$$|\alpha, \beta\rangle = \mathcal{N} \prod_v (\mathbb{1} + \alpha A_v) \prod_p (\mathbb{1} + \beta B_p) |\mathbf{h}\rangle, \quad (\text{B2})$$

where $|\mathbf{h}\rangle$ denotes the state fully polarized in the field direction. When $\mathbf{h} = 0$, the exact ground state is given by $\alpha = \beta = 1$, whereas for $J = 0$, it is obtained for $\alpha = \beta = 0$. Although the normalization constant \mathcal{N} is hard to compute for arbitrary $|\mathbf{h}\rangle$, it is possible to find exact expressions for some particular field directions.

In the following, we focus on two simple directions: the parallel-field case where the field points in the z (or equivalently x) direction [41–43], and the transverse-field case where it points in the y direction. In the former case, a second-order phase transition in the Ising universality class is known to occur for $h_z/J \simeq 0.328$ [41–43], whereas in the latter case, a first-order transition occurs for $h_y/J = 1$ [44]. As we will see, the ansatz state $|\alpha, \beta\rangle$ qualitatively captures these two very different behaviors.

3. Parallel field

For a start, we consider a field $\mathbf{h} = (0, 0, h)$ pointing along the z axis. When J vanishes, the ground state is $|\uparrow\rangle = \otimes_l |\uparrow\rangle_l$, namely, the polarized state where all spins point in the z direction. In the opposite limit where $h = 0$, the system is in the topological (toric code) phase. The ground state is then an eigenstate of all A_v and B_p operators, with eigenvalues 1, that can be written $\mathcal{N} \prod_v (\frac{\mathbb{1} + A_v}{2}) |\uparrow\rangle$. For $h \neq 0$, the Hamiltonian still commutes with all B_p operators and the problem can then be mapped onto an Ising lattice gauge theory on the square lattice [41]. The ground state is an eigenstate of all B_p 's with eigenvalues 1 which enforces $\beta = 1$ in Eq. (B2). Thus, we consider the following simple ansatz state:

$$|\alpha\rangle = |\alpha, \beta = 1\rangle = \mathcal{N} \prod_v (\mathbb{1} + \alpha A_v) |\uparrow\rangle. \quad (\text{B3})$$

The structure of this state is simple enough to allow for straightforward calculations of all quantities appearing in the Hamiltonian.

a. Normalization

Since $A_v^2 = 1$, one has $(\mathbb{1} + \alpha A_v)^2 = (1 + \alpha^2)(\mathbb{1} + \eta A_v)$, where

$$\eta = \frac{2\alpha}{1 + \alpha^2}. \quad (\text{B4})$$

For a finite-size system with N_v vertices and open boundary conditions, the normalization condition thus reads

$$1 = \langle \alpha | \alpha \rangle = \mathcal{N}^2 (1 + \alpha^2)^{N_v} \langle \uparrow | \prod_v (\mathbb{1} + \eta A_v) | \uparrow \rangle. \quad (\text{B5})$$

The only contribution to $\langle \uparrow | \prod_v (\mathbb{1} + \eta A_v) | \uparrow \rangle$ arises from the term proportional to $\mathbb{1}$ (i.e., that does not involve any A_v operator), since an A_v operator for a boundary vertex flip boundary spins. These spin flips cannot be compensated by the action of other A_v operators. As a consequence, the state $|\alpha\rangle$ is normalized if the following condition holds:

$$1 = \langle \alpha | \alpha \rangle = \mathcal{N}^2 (1 + \alpha^2)^{N_v}. \quad (\text{B6})$$

b. Computation of $\langle B_p \rangle_\alpha$ and $\langle A_v \rangle_\alpha$

Since all B_p and all A_v operators commute, it is easy to see that

$$\langle B_p \rangle_\alpha = \langle \alpha | B_p | \alpha \rangle = 1. \quad (\text{B7})$$

The computation of $\langle A_v \rangle_\alpha = \langle \alpha | A_v | \alpha \rangle$ is also straightforward since

$$\begin{aligned} \langle A_v \rangle_\alpha &= \mathcal{N}^2 (1 + \alpha^2)^{N_v} \langle \uparrow | A_v \prod_{v'} (\mathbb{1} + \eta A_{v'}) | \uparrow \rangle \\ &= \langle \uparrow | (\eta \mathbb{1} + A_v) \prod_{v' \neq v} (\mathbb{1} + \eta A_{v'}) | \uparrow \rangle. \end{aligned} \quad (\text{B8})$$

Here, we used the normalization condition (B6) and the fact that $A_v^2 = \mathbb{1}$. As for the calculation of the norm, the only nonzero contribution comes from the term proportional to $\mathbb{1}$, so that one gets

$$\langle A_v \rangle_\alpha = \eta. \quad (\text{B9})$$

This result is independent of N_v and is thus valid in the thermodynamical limit. This will be the case for all quantities discussed below.

c. Computation of $\langle \prod_{v \in \mathcal{V}_n} A_v \rangle_\alpha$

Let \mathcal{V}_n be a set of n vertices. The same argument as above shows that all vertices of \mathcal{V}_n have a contribution η while other vertices have a contribution 1, so that

$$\left\langle \prod_{v \in \mathcal{V}_n} A_v \right\rangle_\alpha = \eta^n = \langle A_v \rangle_\alpha^n. \quad (\text{B10})$$

This factorization property illustrates the mean-field character of the variational state $|\alpha\rangle$.

d. Computation of $\langle \sigma_l^z \rangle_\alpha$

We now turn to the calculation of $\langle \sigma_l^z \rangle_\alpha = \langle \alpha | \sigma_l^z | \alpha \rangle$ at link l :

$$\langle \sigma_l^z \rangle_\alpha = \mathcal{N}^2 \langle \uparrow | \prod_v (\mathbb{1} + \alpha A_v) \sigma_l^z \prod_v (\mathbb{1} + \alpha A_v) | \uparrow \rangle. \quad (\text{B11})$$

We denote v_1 and v_2 the two vertices that share link l . Then $\sigma_l^z A_{v_j} = -A_{v_j} \sigma_l^z$ for $j = 1, 2$, while σ_l^z commutes with all other A_v operators. Using the trivial identity $(\mathbb{1} + \alpha A_{v_j})(\mathbb{1} - \alpha A_{v_j}) = (1 - \alpha^2)\mathbb{1}$, we obtain

$$\langle \sigma_l^z \rangle_\alpha = \mathcal{N}^2 \langle \uparrow | \prod_{v \neq v_1, v_2} (\mathbb{1} + \eta A_v) (1 - \alpha^2)^2 | \uparrow \rangle. \quad (\text{B12})$$

We thus get

$$\langle \sigma_l^z \rangle_\alpha = \left(\frac{1 - \alpha^2}{1 + \alpha^2} \right)^2. \quad (\text{B13})$$

e. Computation of $\langle \sigma_l^x \rangle_\alpha$ and $\langle \sigma_l^y \rangle_\alpha$

For the sake of completeness, let us mention that

$$\langle \sigma_l^x \rangle_\alpha = \langle \sigma_l^y \rangle_\alpha = 0, \quad (\text{B14})$$

which follows from the fact that σ_l^x and σ_l^y both flip a single spin and that this single spin flip cannot be compensated by any product of A_v operators.

f. Computation of the energy per link e

On the square lattice, in the thermodynamical limit, the number of plaquettes N_p equals the number of vertices N_v , and this number is half the number of links N_l of the lattice. As a consequence, the variational energy per link $e(\alpha) = \langle \alpha | H | \alpha \rangle / N_l$ can be written as follows if one gathers all previous results:

$$e(\alpha) = -\frac{J}{2}(\eta + 1) - h \left(\frac{1 - \alpha^2}{1 + \alpha^2} \right)^2. \quad (\text{B15})$$

Denoting $\eta = \frac{2\alpha}{1+\alpha^2} = \cos \theta$ and $\frac{1-\alpha^2}{1+\alpha^2} = \sin \theta$, one finally obtains

$$e(\theta) = -\frac{J}{2}(\cos \theta + 1) - h \sin^2 \theta. \quad (\text{B16})$$

g. Analysis of the variational energy and phase diagram

The variational energy $e(\theta)$ exactly has the form one would obtain by (i) noting that the Hamiltonian is dual to the transverse-field Ising model on the square lattice, thanks to the duality transformation $A_v = \mu_v^z$ and $\sigma_l^z = \mu_{v_1}^x \mu_{v_2}^x$ with v_1 and v_2 being the two adjoining vertices to link l ; (ii) performing a mean-field treatment from the dual spin-1/2 variables μ , namely, by writing the variational state as a product state $|\theta\rangle = \otimes_v |\theta\rangle_v$ satisfying $\langle \mu_v^z \rangle_\theta = \cos \theta$, $\langle \mu_v^x \rangle_\theta = \sin \theta$, and $\langle \mu_{v_1}^x \mu_{v_2}^x \rangle_\theta = \sin^2 \theta$. Of course, a direct mean-field treatment based on the original variables σ cannot describe this transition since a product state is topologically trivial.

The energy $e(\theta)$ can be studied easily. It has a single minimum at $\theta = 0$, i.e., $\alpha = 1$, when $x = h/J \leq x_c = 1/4$. When $x > x_c$, a single minimum is found for $\cos \theta = x_c/x$, thus for $\alpha < 1$. This shows that there is a second-order quantum phase transition at $x = x_c$, between the low-field ($x < x_c$) topological phase, and the high-field ($x > x_c$) polarized phase. The mean-field approach is thus able to capture the qualitative features of the phase transition, since it is known that the transverse-field Ising model has a second-order quantum phase transition at $x_c \simeq 0.328$. However, the position of the critical point is about 24% off since we find $x_c = 1/4$.

It is also interesting to note that, in the topological phase, $e(x < x_c) = -J$, which agrees with the order 1 perturbative expansion in the low-field limit $h/J \ll 1$. In the polarized phase, one has

$$e(x > x_c) = -h - \frac{J}{2} - \frac{J^2}{16h}, \quad (\text{B17})$$

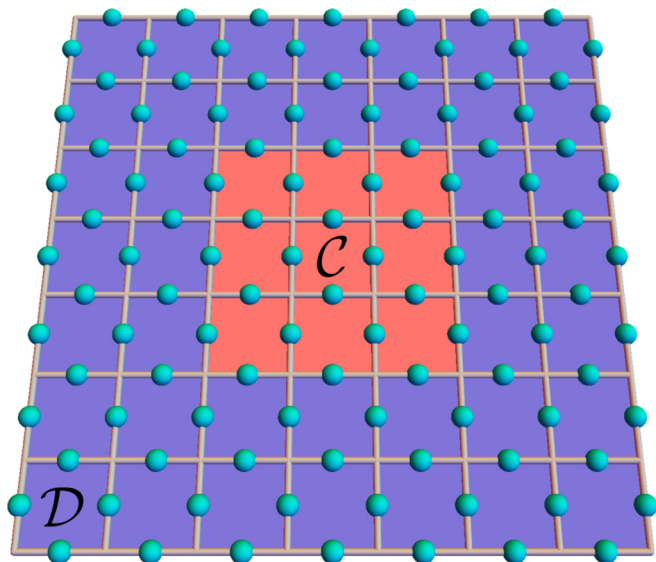


FIG. 4. (Color online) Partition of the lattice between two subsets \mathcal{C} and \mathcal{D} , where \mathcal{C} is simply connected.

which agrees with series expansion up to order 2 in the high-field limit $J/h \ll 1$. As explained for string nets, this is due to the fact that the mean-field ansatz only captures quantum fluctuations at a single-vertex level which is not sufficient to obtain the exact contributions at higher orders.

h. Topological entropy

A reliable way to detect topological order in a given quantum state is to compute the topological entropy [35,36]. In the following, we show that state $|\alpha\rangle$ has a nonvanishing topological entropy only if $\alpha = 1$, which is in agreement with the nature of the phases expected on both sides of the critical point x_c .

As shown in Ref. [45], the topological entropy can be extracted from the computation of the Rényi entanglement entropy. We consider a system with open boundary conditions, and we split it into two subsystems \mathcal{C} and \mathcal{D} , where \mathcal{C} is simply connected, as shown in Fig. 4 for an example where \mathcal{C} has a square shape. We denote c , d , and n the numbers of vertices fully included in \mathcal{C} , fully included in \mathcal{D} , and belonging to both \mathcal{C} and \mathcal{D} , respectively. The aim is to compute the Rényi entanglement entropy between \mathcal{C} and \mathcal{D} when the system is in state $|\alpha\rangle$, namely, $\mathcal{E}_2 = -\log_2[\text{Tr}(\rho_C^2)]$, where $\rho_C = \text{Tr}_D|\alpha\rangle\langle\alpha|$. In the thermodynamical limit, and for a domain \mathcal{C} that becomes bigger and bigger, $\mathcal{E}_2 = \beta n - \gamma + \dots$ where \dots contains all terms that vanish as $n \rightarrow \infty$. The first term is nonuniversal, contrary to the second one $S_{\text{topo}} = -\gamma$, which is the topological entropy. It can be shown that $S_{\text{topo}} = -\log_2 D$, where D is the total quantum dimension of the model under consideration. We shall prove below that

$$S_{\text{topo}}(\alpha = 1) = -1 \quad \text{and} \quad S_{\text{topo}}(0 \leq \alpha < 1) = 0, \quad (\text{B18})$$

so that only the state $|\alpha = 1\rangle$ has topological properties, with the expected quantum dimension $D = 2$, since there are four kinds of Abelian particles in the toric code model [2].

In order to perform this calculation, we begin by rewriting $|\alpha\rangle$ as follows:

$$|\alpha\rangle = \frac{\mathcal{N}}{\mathcal{N}_C \mathcal{N}_D} \prod_{v \in \partial} (\mathbb{1} + \alpha A_v) |\alpha\rangle_C \otimes |\alpha\rangle_D, \quad (\text{B19})$$

where ∂ denotes the boundary of \mathcal{C} and \mathcal{D} , namely, the vertices belonging to both \mathcal{C} and \mathcal{D} , and where

$$|\alpha\rangle_C = \mathcal{N}_C \prod_{v \in \mathcal{C}} (\mathbb{1} + \alpha A_v) |\uparrow\rangle_C \quad \text{with} \quad |\uparrow\rangle_C = \otimes_{l \in \mathcal{C}} |\uparrow\rangle_l, \quad (\text{B20})$$

$$|\alpha\rangle_D = \mathcal{N}_D \prod_{v \in \mathcal{D}} (\mathbb{1} + \alpha A_v) |\uparrow\rangle_D \quad \text{with} \quad |\uparrow\rangle_D = \otimes_{l \in \mathcal{D}} |\uparrow\rangle_l. \quad (\text{B21})$$

These are normalized states, which impose the conditions $\mathcal{N}_C^2 (1 + \alpha^2)^c = 1$ and $\mathcal{N}_D^2 (1 + \alpha^2)^d = 1$, that can be found as before, since \mathcal{C} and \mathcal{D} have (at least) one boundary. Knowing that $\mathcal{N}^2 (1 + \alpha^2)^{c+d+n} = 1$, we can rewrite

$$|\alpha\rangle = \mathcal{M} \prod_{v \in \partial} (\mathbb{1} + \alpha A_v) |\alpha\rangle_C \otimes |\alpha\rangle_D, \quad (\text{B22})$$

with $\mathcal{M}^2 (1 + \alpha^2)^n = 1$.

For each vertex $v \in \partial$, we write $A_v = A_v^C A_v^D$, where the operator $A_v^C = \prod_{l \in v \cap \mathcal{C}} \sigma_l^x$ flips the spins that belong to both v and \mathcal{C} , and where $A_v^D = \prod_{l \in v \cap \mathcal{D}} \sigma_l^x$ is defined similarly with domain \mathcal{D} . Then, state $|\alpha\rangle$ can be expanded as follows:

$$\begin{aligned} |\alpha\rangle = & \mathcal{M} \left(|\alpha\rangle_C \otimes |\alpha\rangle_D + \alpha \sum_{v \in \partial} A_v^C |\alpha\rangle_C \otimes A_v^D |\alpha\rangle_D \right. \\ & + \alpha^2 \sum_{v_1 \neq v_2 \in \partial} A_{v_1}^C A_{v_2}^C |\alpha\rangle_C \otimes A_{v_1}^D A_{v_2}^D |\alpha\rangle_D + \dots \\ & \left. + \alpha^n A_{v_1}^C \dots A_{v_n}^C |\alpha\rangle_C \otimes A_{v_1}^D \dots A_{v_n}^D |\alpha\rangle_D \right), \quad (\text{B23}) \end{aligned}$$

where in the last term, all v_1, \dots, v_n are distinct and belong to ∂ .

For open boundary conditions, the states $|\alpha\rangle_D$, $\{A_v^D |\alpha\rangle_D, v \in \partial\}$, $\{A_{v_1}^D A_{v_2}^D |\alpha\rangle_D, v_1 \neq v_2 \in \partial\}$, \dots , $\{A_{v_1}^D \dots A_{v_n}^D |\alpha\rangle_D$ are all different and form an orthonormal set of states. It is thus easy to take the partial trace needed to compute the reduced density matrix $\rho_C = \text{Tr}_D |\alpha\rangle\langle\alpha|$. One gets

$$\begin{aligned} \rho_C = & \mathcal{M}^2 \left(|\alpha\rangle_C \langle\alpha| + \alpha^2 \sum_{v \in \partial} A_v^C |\alpha\rangle_C \langle\alpha| A_v^C + \dots \right. \\ & \left. + \alpha^{2n} A_{v_1}^C \dots A_{v_n}^C |\alpha\rangle_C \langle\alpha| A_{v_1}^C \dots A_{v_n}^C \right), \quad (\text{B24}) \end{aligned}$$

where we did not write as many terms as before to keep things as readable as possible.

To compute $\text{Tr}(\rho_C^2)$, one needs to find the spectrum of ρ_C . For this, one has to see that all states appearing in the expression of ρ_C , namely, $|\alpha\rangle_C$, $\{A_v^C |\alpha\rangle_C, v \in \partial\}$, $\{A_{v_1}^C A_{v_2}^C |\alpha\rangle_C, v_1 \neq v_2 \in \partial\}$, \dots , $\{A_{v_1}^C \dots A_{v_n}^C |\alpha\rangle_C$ are normed but not orthogonal to each other, because one has the following

identity:

$$A_{v_1}^c \cdots A_{v_n}^c = \prod_{v \in \mathcal{C}} A_v. \quad (\text{B25})$$

Indeed, let us define two complementary states $|\psi_1\rangle_{\mathcal{C}}$ and $|\psi_2\rangle_{\mathcal{C}}$, as states from the set written above that have the overlap

$$\begin{aligned} {}_c\langle\psi_1|\psi_2\rangle_{\mathcal{C}} &= {}_c\langle\alpha|A_{v_1}^c \cdots A_{v_n}^c|\alpha\rangle_{\mathcal{C}} = {}_c\langle\alpha|\prod_{v \in \mathcal{C}} A_v|\alpha\rangle_{\mathcal{C}} \\ &= \eta^c, \end{aligned} \quad (\text{B26})$$

the last expression being obtained as Eq. (B10). Thus, two complementary states are not orthogonal. On the contrary, two states that are not complementary are easily seen to be orthogonal. As a consequence, the density matrix $\rho_{\mathcal{C}}$ has a block diagonal structure. Each block is a 2×2 matrix involving two complementary states, of the form

$$\rho_{\mathcal{C}}^{(j)} = \mathcal{M}^2(\alpha^{2j}|\psi_1\rangle_{\mathcal{C}}{}_c\langle\psi_1| + \alpha^{2(n-j)}|\psi_2\rangle_{\mathcal{C}}{}_c\langle\psi_2|), \quad (\text{B27})$$

where j is the number of A_v^c operators appearing in state $|\psi_1\rangle_{\mathcal{C}} = A_{v_1}^c \cdots A_{v_j}^c|\alpha\rangle$, with $0 \leq j \leq n/2$. For the sake of simplicity, we shall consider that n is an even number, as is the case in Fig. 4. When $j < n/2$, there are $\binom{n}{j}$ such $\rho_{\mathcal{C}}^{(j)}$ matrices. When $j = n/2$, there are $\frac{1}{2}\binom{n}{n/2}$ matrices $\rho_{\mathcal{C}}^{(n/2)}$.

The matrices $\rho_{\mathcal{C}}^{(j)}$ can be rewritten in an orthonormal basis made of states $|\phi_1\rangle_{\mathcal{C}}$ and $|\phi_2\rangle_{\mathcal{C}}$. For this, one first computes the overlap matrix \mathcal{O} with matrix elements $\mathcal{O}_{k,l} = {}_c\langle\psi_k|\psi_l\rangle_{\mathcal{C}}$ with k and l taking values 1 or 2, namely,

$$\mathcal{O} = \begin{pmatrix} 1 & \eta^c \\ \eta^c & 1 \end{pmatrix}. \quad (\text{B28})$$

This symmetric matrix can be diagonalized by performing a rotation, $\mathcal{O} = {}^t\mathcal{P}\mathcal{D}\mathcal{P}$, with

$$\mathcal{P} = \frac{1}{\sqrt{2}} \begin{pmatrix} -1 & 1 \\ 1 & 1 \end{pmatrix} \quad \text{and} \quad \mathcal{D} = \begin{pmatrix} 1 - \eta^c & 0 \\ 0 & 1 + \eta^c \end{pmatrix}. \quad (\text{B29})$$

With these definitions, and noting that the diagonal matrix \mathcal{D} has non-negative diagonal elements, one can perform the change of basis

$$\begin{pmatrix} |\psi_1\rangle_{\mathcal{C}} \\ |\psi_2\rangle_{\mathcal{C}} \end{pmatrix} = {}^t\mathcal{P}\mathcal{D}^{1/2}\mathcal{P} \begin{pmatrix} |\phi_1\rangle_{\mathcal{C}} \\ |\phi_2\rangle_{\mathcal{C}} \end{pmatrix}. \quad (\text{B30})$$

One can then express $\rho_{\mathcal{C}}^{(j)}$ in the orthonormal basis of states $|\phi_1\rangle_{\mathcal{C}}$ and $|\phi_2\rangle_{\mathcal{C}}$ (the expressions being quite large, we shall not give them here).

A check of the validity of the obtained expression is to compute $\text{Tr}\rho_{\mathcal{C}}$. We find that

$$\text{Tr}(\rho_{\mathcal{C}}^{(j)}) = \frac{\alpha^{2j} + \alpha^{2(n-j)}}{(1 + \alpha^2)^n}, \quad (\text{B31})$$

$$\text{thus} \quad \text{Tr}\rho_{\mathcal{C}} = \frac{1}{2} \sum_{j=0}^n \binom{n}{j} \text{Tr}(\rho_{\mathcal{C}}^{(j)}) = 1, \quad (\text{B32})$$

as it should. Note that we have extended the sum over $j = 0, \dots, n/2$ to $j = 0, \dots, n$ and have corrected the induced double counting by the prefactor $1/2$.

Similarly, one can compute $\text{Tr}(\rho_{\mathcal{C}}^{(j)^2})$ and deduce

$$\begin{aligned} \text{Tr}(\rho_{\mathcal{C}}^2) &= \frac{1}{2} \sum_{j=0}^n \binom{n}{j} \text{Tr}(\rho_{\mathcal{C}}^{(j)^2}) \\ &= \left[\frac{1 + \alpha^4}{(1 + \alpha^2)^2} \right]^n \left[1 + \left(\frac{2\alpha^2}{1 + \alpha^4} \right)^n \left(\frac{2\alpha}{1 + \alpha^2} \right)^{2c} \right]. \end{aligned} \quad (\text{B33})$$

In the case $\alpha = 1$, one finds $\text{Tr}(\rho_{\mathcal{C}}^2) = 2^{1-n}$, so that $\mathcal{E}_2(\alpha = 1) = n - 1$ and $S_{\text{topo}} = -1$, as expected [35,36]. When $0 \leq \alpha < 1$, the second term in the above equation vanishes exponentially fast when n grows (for a generic domain \mathcal{C} , c grows like n^2). One then gets the following behavior of \mathcal{E}_2 :

$$\mathcal{E}_2 = n \log_2 \left[\frac{(1 + \alpha^2)^2}{1 + \alpha^4} \right] + \dots, \quad (\text{B34})$$

where \dots represents terms that vanish when taking the limit $n \rightarrow \infty$. As a consequence, the topological entropy vanishes when $0 \leq \alpha < 1$.

i. Wilson loops

As already mentioned, the topological phase ($x < x_c$) is the deconfined phase of the Ising lattice gauge model, in which Wilson loops are known to obey a perimeter law [46]. By contrast, in the polarized (deconfined) phase, these loops obey an area law. In the toric code model, Wilson loop operators $W_{\mathcal{C}}$ can be chosen as a product of σ_j^x operators along a closed contour, which is nothing but the product of all operators A_v surrounded by this contour. Using Eq. (B10), one thus gets $\langle W_{\mathcal{C}} \rangle_{\alpha} = \eta^n$ where $\eta = \cos \theta = \frac{2\alpha}{1 + \alpha^2}$. In the topological phase, the energy is minimized for $\alpha = 1$ so that $\langle W_{\mathcal{C}} \rangle_{\alpha} = 1$ for any contour \mathcal{C} . This can be interpreted as a trivial perimeter law with an infinite characteristic length. In the polarized phase ($\alpha < 1$), one can write $\langle W_{\mathcal{C}} \rangle = \exp[-n \ln(1/\eta)]$, which is an area law with a characteristic area $1/\ln(1/\eta)$. Our variational state thus correctly mimics the expected behavior of W in the deconfined phase as well as in the confined phase.

4. Transverse field

We now consider a field $\mathbf{h} = (0, h, 0)$ pointing along the y axis. In this case, the model is known to display a first-order quantum phase transition at the self-dual point $h = J$ [44]. The variational state reads

$$|\alpha, \beta\rangle = \mathcal{N} \prod_v (\mathbb{1} + \alpha A_v) \prod_p (\mathbb{1} + \beta B_p) |\Rightarrow\rangle, \quad (\text{B35})$$

where $|\Rightarrow\rangle = \otimes_l |\rightarrow\rangle_l$ is the polarized state where all spins point in the y direction. For the sake of completeness, we introduced two variational parameters α and β but, for symmetry reasons, we expect them to be equal.

Since all calculations follow closely that of the preceding section, we shall directly give the results without further justification. The expectation values of charge and flux operators read

$$\langle A_v \rangle_{\alpha, \beta} = \frac{2\alpha}{1 + \alpha^2} \quad \text{and} \quad \langle B_p \rangle_{\alpha, \beta} = \frac{2\beta}{1 + \beta^2}. \quad (\text{B36})$$

In addition, one has $\langle \sigma_l^x \rangle_{\alpha, \beta} = 0$, $\langle \sigma_l^z \rangle_{\alpha, \beta} = 0$, and

$$\langle \sigma_l^y \rangle_{\alpha, \beta} = \left(\frac{1 - \alpha^2}{1 + \alpha^2} \right)^2 \left(\frac{1 - \beta^2}{1 + \beta^2} \right)^2. \quad (\text{B37})$$

Setting $\cos \theta = \frac{2\alpha}{1+\alpha^2}$, $\sin \theta = \frac{1-\alpha^2}{1+\alpha^2}$ and $\cos \phi = \frac{2\beta}{1+\beta^2}$, $\sin \phi = \frac{1-\beta^2}{1+\beta^2}$, and keeping in mind that, in the thermodynamical limit, $N_v = N_p = N_l/2$, one gets the following energy per link:

$$e(\theta, \phi) = -\frac{J}{2} \cos \theta - \frac{J}{2} \cos \phi - h \sin^2 \theta \sin^2 \phi. \quad (\text{B38})$$

As expected, this variational energy is found to be minimum for $\phi = \theta$, i.e., for $\alpha = \beta$. Again, the expression of $e(\theta, \theta)$ could have been obtained by using a duality transformation and treating the dual model in a mean-field way. The study of $e(\theta, \theta)$ shows that $\theta = 0$ is always a minimum, but is the absolute minimum only for $x = h/J < x_c = 27/32$. For

$x \geq x^* = \frac{3\sqrt{3}}{8}$, a second local minimum appears and it becomes the absolute minimum for $x > x_c$. For $x = x_c$, two absolute minima coexist, at $\theta = 0$ and at $\theta = \arccos(1/3)$. We thus find a first-order quantum phase transition at $x = x_c$. Consequently, our variational analysis is thus about 16% off the exact result $x_c = 1$, and misses the self-duality of the model [44].

Finally, in the topological phase, $e(x < x_c) = -J$ agrees with the low-field series expansion up to order 1 in h/J . In the polarized phase, the series expansion of the variational energy at order 4 in J/h reads

$$e(x < x_c) = -h - \frac{J^2}{8h} - \frac{J^4}{256h^3}, \quad (\text{B39})$$

which matches the high-field series expansion up to order 2 in J/h [44] (odd order contributions vanish).

-
- [1] X.-G. Wen, *ISRN Condens. Matter Phys.* **2013**, 198710 (2013).
[2] A. Y. Kitaev, *Ann. Phys. (NY)* **303**, 2 (2003).
[3] See <http://www.theory.caltech.edu/people/preskill/ph219/> for a pedagogical introduction.
[4] Z. Wang, *Topological Quantum Computation*, CBMS Regional Conference Series in Mathematics, Number 112 (American Mathematical Society, Providence, 2010).
[5] C. Nayak, S. H. Simon, A. Stern, and M. Freedman, *Rev. Mod. Phys.* **80**, 1083 (2008).
[6] S. Bravyi, M. B. Hastings, and S. Michalakis, *J. Math. Phys.* **51**, 093512 (2010).
[7] M. A. Levin and X.-G. Wen, *Phys. Rev. B* **71**, 045110 (2005).
[8] C.-H. Lin and M. Levin, *Phys. Rev. B* **89**, 195130 (2014).
[9] C. Gils, S. Trebst, A. Kitaev, A. W. W. Ludwig, M. Troyer, and Z. Wang, *Nat. Phys.* **5**, 834 (2009).
[10] F. J. Burnell, S. H. Simon, and J. K. Slingerland, *Phys. Rev. B* **84**, 125434 (2011).
[11] M. D. Schulz, S. Dusuel, R. Orús, J. Vidal, and K. P. Schmidt, *New J. Phys.* **14**, 025005 (2012).
[12] V. Karimipour, L. Memarzadeh, and P. Zarkeshian, *Phys. Rev. A* **87**, 032322 (2013).
[13] R. Mohseninia, S. S. Jahromi, L. Memarzadeh, and V. Karimipour, *Phys. Rev. B* **91**, 245110 (2015).
[14] M. D. Schulz (unpublished).
[15] H.-X. He, C. J. Hamer, and J. Oitmaa, *J. Phys. A* **23**, 1775 (1990).
[16] C. J. Hamer, J. Oitmaa, and Z. Weihong, *J. Phys. A* **25**, 1821 (1992).
[17] M. D. Schulz, S. Dusuel, K. P. Schmidt, and J. Vidal, *Phys. Rev. Lett.* **110**, 147203 (2013).
[18] M. D. Schulz, S. Dusuel, G. Misguich, K. P. Schmidt, and J. Vidal, *Phys. Rev. B* **89**, 201103 (2014).
[19] K. G. Wilson, *Phys. Rev. D* **10**, 2445 (1974).
[20] F. Y. Wu, *Rev. Mod. Phys.* **54**, 235 (1982).
[21] P. A. Pearce, *Physica A* **125**, 247 (1984).
[22] C. Gils, *J. Stat. Mech.* (2009) P07019.
[23] E. Ardonne, J. Gukelberger, A. W. W. Ludwig, S. Trebst, and M. Troyer, *New J. Phys.* **13**, 045006 (2011).
[24] M. D. Schulz, S. Dusuel, and J. Vidal, *Phys. Rev. B* **91**, 155110 (2015).
[25] Z.-C. Gu, M. Levin, B. Swingle, and X.-G. Wen, *Phys. Rev. B* **79**, 085118 (2009).
[26] O. Buerschaper, M. Aguado, and G. Vidal, *Phys. Rev. B* **79**, 085119 (2009).
[27] Z.-C. Gu, M. Levin, and X.-G. Wen, *Phys. Rev. B* **78**, 205116 (2008).
[28] S. Dusuel, M. Kamfor, R. Orús, K. P. Schmidt, and J. Vidal, *Phys. Rev. Lett.* **106**, 107203 (2011).
[29] F. Liu and X.-G. Wen, [arXiv:1504.08365](https://arxiv.org/abs/1504.08365).
[30] R. N. C. Pfeifer, P. Corboz, O. Buerschaper, M. Aguado, M. Troyer, and G. Vidal, *Phys. Rev. B* **82**, 115126 (2010).
[31] X. Chen, B. Zeng, Z.-C. Gu, I. L. Chuang, and X.-G. Wen, *Phys. Rev. B* **82**, 165119 (2010).
[32] O. Buerschaper, J. M. Mombelli, M. Christandl, and M. Aguado, *J. Math. Phys.* **54**, 012201 (2013).
[33] B. Swingle and X.-G. Wen, [arXiv:1001.4517](https://arxiv.org/abs/1001.4517).
[34] N. Schuch, I. Cirac, and D. Pérez-García, *Ann. Phys. (NY)* **325**, 2153 (2010).
[35] A. Kitaev and J. Preskill, *Phys. Rev. Lett.* **96**, 110404 (2006).
[36] M. Levin and X.-G. Wen, *Phys. Rev. Lett.* **96**, 110405 (2006).
[37] R. Orús, T. C. Wei, O. Buerschaper, and M. V. den Nest, *New J. Phys.* **16**, 013015 (2014).
[38] R. Orús, T. C. Wei, O. Buerschaper, and A. García-Saez, *Phys. Rev. Lett.* **113**, 257202 (2014).
[39] M. Levin and X.-G. Wen, *Phys. Rev. B* **75**, 075116 (2007).
[40] P. H. Bonderson, Ph.D. thesis, California Institute of Technology, 2007.
[41] S. Trebst, P. Werner, M. Troyer, K. Shtengel, and C. Nayak, *Phys. Rev. Lett.* **98**, 070602 (2007).
[42] A. Hamma and D. A. Lidar, *Phys. Rev. Lett.* **100**, 030502 (2008).
[43] J. Vidal, S. Dusuel, and K. P. Schmidt, *Phys. Rev. B* **79**, 033109 (2009).
[44] J. Vidal, R. Thomale, K. P. Schmidt, and S. Dusuel, *Phys. Rev. B* **80**, 081104 (2009).
[45] S. T. Flammia, A. Hamma, T. L. Hughes, and X.-G. Wen, *Phys. Rev. Lett.* **103**, 261601 (2009).
[46] L. Tagliacozzo and G. Vidal, *Phys. Rev. B* **83**, 115127 (2011).